Polyimide-Silica Nanocomposites Exhibiting Low Thermal Expansion Coefficient and Water Absorption from Surface-Modified Silica

J. C. Tang,[1,2] G. L. Lin,[1] H. C. Yang,[2] G. J. Jiang,[1] Y. W. Chen-Yang[1]

[1]*Department of Chemistry, Center for Nanotechnology and R & D Center for Membrane Technology, Chung Yuan Christian University, Chung-Li 320, Taiwan, Republic of China*
[2]*Department of Environment Engineering, Chin Min Institute of Technology, Tou-Fen, Miao-Li 351, Taiwan, Republic of China*

Received 28 January 2006; accepted 14 September 2006
DOI 10.1002/app.26041
Published online in Wiley InterScience (www.interscience.wiley.com).

ABSTRACT: In this study, a commercially available nano-sized silica (SiO_2) was surface-modified via esterification with oleic acid (OA), a relatively inexpensive and hydrophobic modifier, and characterized by FTIR, NMR, SEM, EDS, and TGA measurements. Various amounts of the surface-modified silica nanoparticles (SiO_2-OA) were dispersed in a poly(amic acid), which were then cyclized at high temperatures to form a series of PI/SiO_2-OA nanocomposite films (PISA). The effect of the addition of the SiO_2-OA nanoparticles on the properties of the as-prepared polyimide nanocomposite was studied. The results indicated that, comparing with pure PI and PI/pristine-SiO_2 composite film (PISI), the as-prepared PISA films had enhanced dynamic mechanical properties and thermal stability, as well as reduced water absorption and thermal expansion. The as-prepared PI/SiO_2-OA nanocomposites have potential for applications in high performance microelectronic devices. © 2007 Wiley Periodicals, Inc. J Appl Polym Sci 104, 4096–4105, 2007

Key words: silica; nanoparticles; polyimide; nanocomposites; water absorption

INTRODUCTION

Since poly(4,4′-oxydiphenylene pyromellitimide) was introduced in the early 1960s, many aromatic polyimides with some desirable characteristics such as excellent mechanical properties, high-temperature stability, low dielectric constant, high breakdown voltage, inertness to solvents, and easy processability, have been prepared and used widely for microelectronic devices, films, adhesives, and in the membrane industry.[1–5] However, most polyimides exhibit relatively high water absorption and coefficients of thermal expansion (CTE) (about 25–50 $\times$ 10^{-6} K^{-1})[6] and limit their applications for advanced electronic products.[2,7–10] Therefore, many studies of PI/inorganic-filler composites, which included PI/oxo-metal nanocomposites,[11,12] PI/metal-complex nanocomposites,[13] PI/organo-clay nanocomposites,[14–17] PI/silica nanocomposites,[18–24] etc., have been studied. Among them, most of the PI/silica nanocomposites reported have been prepared via the sol-gel process, where silica nanoparticles were formed in the polyimide matrices via hydrolysis and polycondensation from the organic-silanes.[18–25] In the studies, several approaches have been used to prevent phase separation between the PI matrix and the silica domain. Those approaches include functionalization of organic-silane precursors, the addition of coupling agents, or combinations of the two approaches; and they have been used to increase the compatibility of the PI matrix and the inorganic phase. Nevertheless, because of the incomplete condensation reaction in the sol-gel process, the as-prepared PI/silica hybrid thin films usually have exhibited lower decomposition temperature (T_d) in higher inorganic contents.[22,23] Furthermore, the organic-silane precursors used for the sol-gel process, such as 3-methacryloxypropyltrimethoxysilane, 4-vinylphenethyltrimethoxysilane, 3-aminopropyltriethoxysilane,[18–24] and γ-glycidyl-oxypropyltrimethoxysilanes[22] are all pricey materials, making this technique not currently industrially practical. Although physically blending of nano-sized SiO_2 particles into a PI matrix is an easier and cheaper method than the sol-gel technique, the enhancement of the compatibility between the silica particles and the PI polymer matrix is still an important issue to be resolved.[25]

Correspondence to: Y. W. Chen-Yang (yuiwhei@cycu.edu.tw).

Contract grant sponsor: National Science Council of Republic of China, Asia Electronic Material Company (Taiwan); contract grant number: NSC92-2113-M-033-020-CC3.

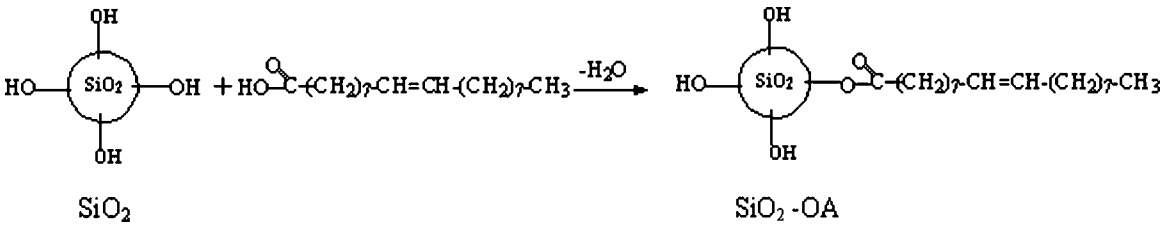

Scheme 1

In this study, instead of the more costly modifiers, an inexpensive modifier, *cis*-9-octadecenoic acid (oleic acid), which contains a long alkyl chain, was used to modify the surface of the nano-scaled silica particles. The OA modified silica (SiO_2-OA) was then dispersed in the polyamic acid and cyclized via a thermal curing process to prepare the corresponding PI/SiO_2-OA hybrid composites (PISA). The effects of the content of SiO_2-OA on the thermal stabilities, mechanical properties, thermal-expansion coefficients (CTE), and capacity of water absorption of the PISA films were investigated and compared with that of pure PI film and PI/pristine SiO_2 composite (PISI) film.

EXPERIMENTAL

Materials

Cis-9-octadecenoic acid (oleic acid, OA), ethanol, and *n*-hexane were obtained from Showa Company. *N*,*N*-dimethylacetamide (DMAC) was obtained from Tediainc Company. 4,4′-diaminodiphenyl ether (ODA) and pyromellitic anhydride (PMDA) were obtained from Chriskev Company. The SiO_2 nanoparticles with diameter of about 12 nm (AIRSOL 200) were obtained from Degussa Company.

Preparation of SiO_2-OA nanoparticles

To modify the SiO_2 nanoparticles, the process depicted in Scheme 1 was used.[26] First, 200 mL *n*-hexane and 3.0 g of SiO_2 nanoparticles were mixed in a three-neck flask equipped with a thermometer and a stirrer, and an appropriate amount of OA was added into the solution. The mixture was heated under vigorous stirring at 60°C for 4 h. It was cooled at −10°C for about 3 h, then filtered with filter paper to obtain the white precipitate. Finally, the precipitate was rinsed thoroughly with the mixture of ethanol and deionized water (3/7 in volume) and dried in a vacuum at 110°C for 10 h. The white powder obtained was identified as the OA surface-modified silica nanoparticles (abbreviated as SiO_2-OA). By changing the ratio of OA to SiO_2 nanoparticles, a series of samples were prepared, and the recipes are shown in Table I.

Measurement of the dispersion stability of SiO_2-OA in the solvents

0.05 g of the fine ground SiO_2-OA powder was added in 20 mL of the solvent listed in Table II. The solution was mixed using ultrasonic equipment for 10 min at room temperature, then left to stand for precipitation. The precipitation time, t_p, was measured as the time required for the precipitates to appear after standing. According to the length of t_p, the dispersion stability of the SiO_2-OA nanoparticles in the solvent were classified into undispersed, partially-dispersed, mostly-dispersed, and well-dispersed as footnoted in Table II.

Preparation of poly(amic acid) (PAA) solution

A diamine solution, 0.06 mol (12.0 g) of ODA in 142.2 g of DMAC (15 wt % solid content), was placed into a 500 mL three-necked round bottomed flask equipped with a thermometer, magnetic stirrer, and nitrogen inlet-outlet system. An equivalent of PMDA 0.06 mol (13.1 g) was slowly added into the well-mixed ODA solution at 15°C for 1 h and stirred at room temperature for 4 h. The reaction solution was then kept in a freezer to prevent any further reaction.

TABLE I
Recipe and TGA Data of the SiO_2-OA Nanoparticle

Sample	SiO_2(g)	OA (g)	$T_{5wt\ \%}$ (°C)	Char yield at 500°C (wt%)	Modifier agent content (wt %)[a]
SiO_2-OA-1	3	1.4	–	95.5	4.5
SiO_2-OA-2	3	7.1	245.3	87.1	12.9
SiO_2-OA-3	3	14.1	227.4	70.6	29.4
SiO_2-OA-4	3	42.0	232.8	49.9	50.1

[a] Modifier agent content (wt %) = 100% − wt % of residue remained at 500°C.

TABLE II
Dispersion Stability of the SiO_2-OA Nanoparticles in Various Solvents[a]

Sample	*n*-Hexane	CCl_4	Alcohol	Water	DMAC
SiO_2	+	+	++++	++++	++++
SiO_2-OA-1	++	++	+++	++	++++
SiO_2-OA-2	+++	+++	+++	++	++++
SiO_2-OA-3	++++	++++	+++	+	+++
SiO_2-OA-4	++++	++++	++	+	+++

[a] + (undispersed), $t_p < 30$ s; ++ (partially-dispersed), 30 s $< t_p <$ 3 min; +++ (mostly-dispersed), 3 min $< t_p <$ 30 min; ++++ (well-dispersed), $t_p > 30$ min.

Preparation of the hybrid nanocomposite films

To prepare the SiO_2-OA-containing PI nanocomposite films, the PAA solution prepared above was diluted with DMAC to form a 10 wt % PAA solution. The solution was then mixed with an appropriate amount of the SiO_2-OA nanoparticles and further stirred for 24 h and with the aid of an ultrasonic bath for 10 min, yielding the PAA/SiO_2-OA homogenous solution. The as-prepared PAA and PAA/SiO_2-OA solutions were separately cast on clean glass substrates by the casting technique to form the corresponding films. The as-prepared films were imidized at 150°C for 2 h, 200°C for 2 h, 250°C for 2 h, and 300°C for 2 h. Finally, the films were cooled to 30°C at a rate of 5°C min^{-1} to obtain the corresponding PI and PI/SiO_2-OA films (PISA). Besides, for comparison, a PI/pristine-SiO_2 hybrid film (PISI) was also prepared in the similar process with addition of 5 wt % pristine SiO_2 in the PAA solution as the filler. The corresponding recipe and the abbreviation of the films are listed in Table III. All these films were characterized with FTIR, TGA, DMA, TMA, EDS, SEM, water absorption, and dielectric constant measurements.

Instruments

The Fourier transform infrared (FTIR) spectra of the SiO_2-OA nano-particles and the as-prepared films were recorded with a BIO-RAD FTS-7 spectrometer. The solid state ^1H NMR spectrum of the SiO_2-OA nanoparticles was recorded with BRUKER DSX-400WB NMR SPECTROMETER, NMR/Solid 400. Thermogravimetric analyses of the SiO_2-OA nanoparticles and the films prepared were performed under nitrogen flow using a SEIKO TG/DTA220 thermogravimetric analyzer at a heating rate of 10°C min^{-1}. The mechanical properties (storage modulus and tan δ) of the films prepared were measured by a DMA-TAQ880 dynamic mechanical analyzer. The surface morphologies, the silicon mapping photographs, and the elemental compositions were investigated on a JSM-6700F field emission scanning electron microscopy (SEM) with an energy dispersive X-ray spectrometry (EDS) analyzer. The samples were coated with platinum using a sputter coater to avoid charging. The dielectric constants of the as-prepared films were determined from the capacitance values using a capacitance meter (Precision Impedance Analyzer-4294A) in 1 MHz at 30°C. A TMA 2940 thermomechanical analyzer was used to measure the linear coefficient of thermal expansion (CTE) of the films prepared. The films prepared (roughly 35 μm thickness) were cut into 2 mm × 22 mm pieces and mounted between two vertical clamps in tension under a force of 0.05 *N*. The samples were heated from room temperature to 350°C at a heating rate of 5°C min^{-1}. The CTE values of the films were obtained over the temperature range of 100–250°C by averaging three test results. The water absorption values of the films prepared were determined at 30°C. The films were vacuum-dried at 100°C for 24 h before testing of the water absorption, for which they were weighed and immersed in deionized water at room temperature for 24 h. The wet films were wiped dry and quickly weighed again. The water absorption of the films was calculated in weight percent as follows:[27]

$$\text{Water absorption} = [(W_2 - W_1)/W_1] \times 100\%$$

where, W_2 = weight of film after absorption water, W_1 = weight of dry film

TABLE III
Recipe and Thermal data of Pure PI and the Hybrid Composite Film

Sample	PAA (g)	SiO_2-OA-1 (g)	SiO_2 (g)	$T_{5\ wt\ \%}$ (°C)[a]	T_{max} (°C)[b]	Residue at 800°C (wt %)[c]	T_g (°C)
PI	18	0	–	549	552	57.1	394
PISI	18	–	0.108	548	552	59.51	394
PISA-3	18	0.054	–	550	555	58.6	395
PISA-5	18	0.108	–	552	552	60.3	395
PISA-7	18	0.126	–	551	552	58.1	395
PISA-9	18	0.162	–	553	551	61.3	394

[a] Temperature at 5% weight loss.
[b] Temperature at maximum weight loss rate.
[c] Char residue remained at 800°C in N_2 atmosphere.

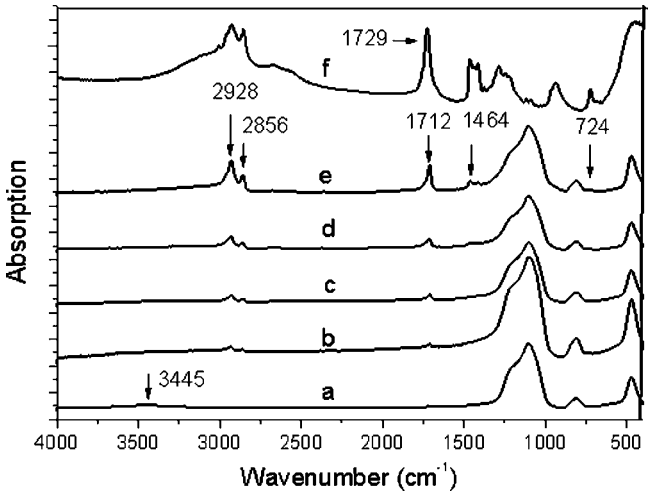

Figure 1 FTIR spectra of (a) pristine SiO_2, (b) SiO_2-OA-1, (c) SiO_2-OA-2, (d) SiO_2-OA-3, (e) SiO_2-OA-4 particles, and (f) oleic acid.

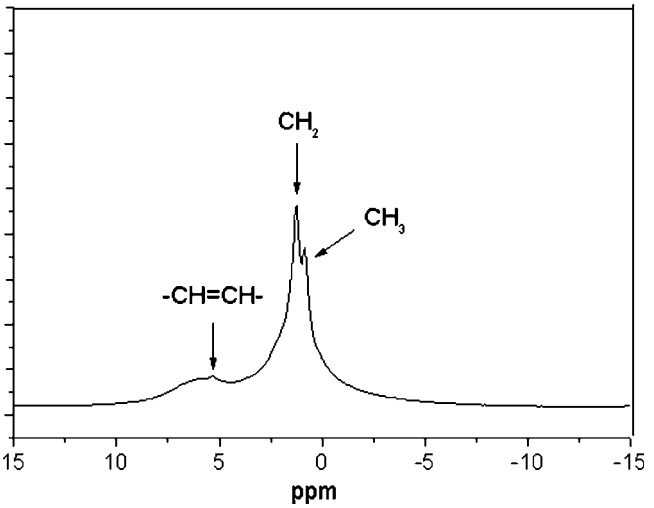

Figure 2 Solid state ^1H NMR of SiO_2-OA-2.

RESULTS AND DISCUSSION

Characterization of the SiO_2-OA nanoparticles

The characteristic groups on the surface of the SiO_2 nanoparticles before and after modification by OA were identified by FTIR spectra. As shown in Figure 1, the Si—O—Si absorption peak is observed at 1080 cm^{-1} for the SiO_2 and SiO_2-OA spectra. The characteristic peak of —COOH of OA at 1729 cm^{-1} disappeared as described in Ref. 26. The absorptions from the stretching of the carboxylate and the rocking of the long alkyl chain are observed at 1712 and 724 cm^{-1}, respectively. Furthermore, the peaks at 2928, 2856, and 1464 cm^{-1} are also found in the spectra of the SiO_2-OA samples for the absorptions of the $—CH_2—$ asymmetrical stretching, symmetrical stretching, and scissoring vibrations, respectively, indicating that the OA has successfully modified the surface of the SiO_2 nanoparticles by reacting the carboxylatic acid groups with the Si—OH groups, which peaked at 3445 cm^{-1}, via the esterification. Moreover, the intensities of these OA peaks are increased with increasing the fed amount of OA, implying that the extent of the modification of OA on the SiO_2 nanoparticle surface can be controlled by the amount of OA fed. Furthermore, as indicated in Figure 2 the spectrum of the solid state ^1H NMR of SiO_2-OA-2 shows three major peaks. The signal at 0.83 ppm is assigned to the protons of the terminal methyl group. The broad peak at 1.32 ppm is assigned to the protons of the methylene groups of

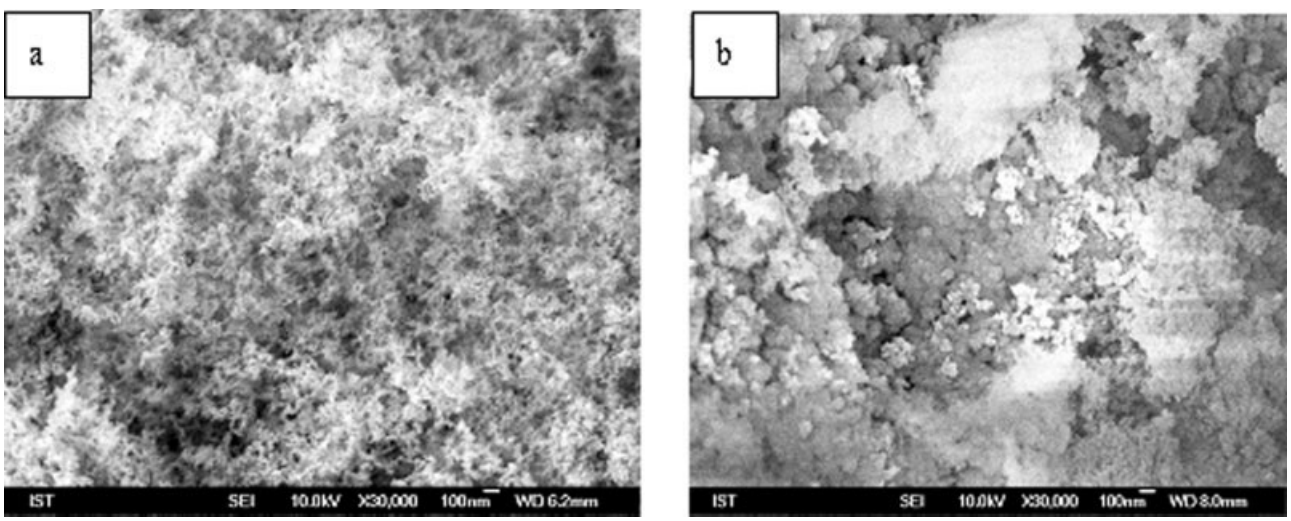

Figure 3 SEM photographs of (a) pristine SiO_2 and (b) SiO_2-OA-1 nanoparticles.

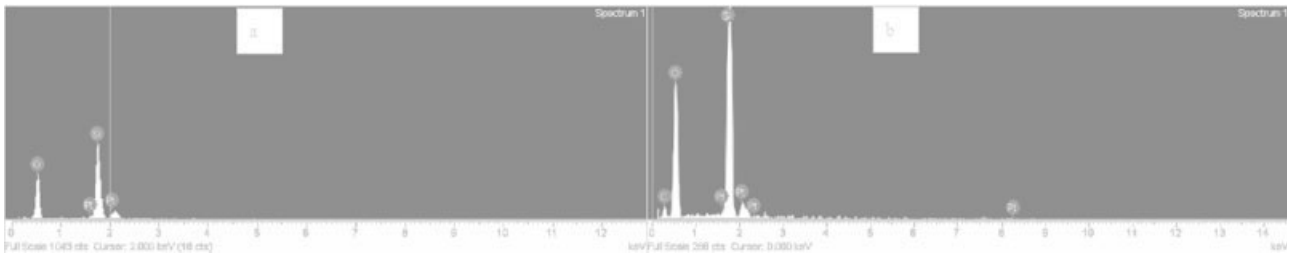

Figure 4 EDS analysis of (a) pristine SiO_2 and (b) SiO_2-OA-1 nanoparticles.

OA, which cannot be resolved, while the peak at 5.28 ppm corresponds to the vinyl protons of OA chain. The result supports that the OA groups were successfully bonded to the surface of the SiO_2 nanoparticles.

Figure 3 shows the SEM photographs of the pristine SiO_2 and SiO_2-OA-1 nanoparticles. It is seen that the SiO_2 nanoparticles purchased were in a homogeneous and loose form with sizes of about 12 nm as mentioned in experimental section provided by the company. On the other hand, the aggregation was found for the SiO_2-OA-1 nanoparticles and is ascribed to the interaction between the C=O groups of the attached OA moities and the unmodified O—H groups on the silica surface. Besides, the corresponding elemental compositions of the pristine SiO_2 and SiO_2-OA-1 nanoparticles obtained by the EDS analysis are shown in Figure 4. As can be observed, except for the peaks of Si and O atoms, the carbon peak is also found for SiO_2-OA-1, providing additional evidence for the presence of the alkyl moiety on the surface of the SiO_2-OA-1 nanoparticles.

Figure 5 shows the TGA curves for the pristine SiO_2 and the SiO_2-OA nanoparticles. The data summarized in Table I indicates that the weight loss of the SiO_2-OA nanoparticles detected at 500°C in nitrogen increases with increasing the fed amount of OA, implying that the more OA was fed the more OA moieties were bonded on the SiO_2 surface, resulting in the lower residual at 500°C. In addition, as indicated in Table II, the dispersion stability of the SiO_2-OA nanoparticles was increased in the nonpolar solvents and decreased in the polar solvents with increasing the OA content. This is attributed to the presence of the OA moieties, which enhanced the hydrophobicity of the nanoparticle's surface. Since the degradation temperature of SiO_2-OA ($T_{5\%}$) was less than 300°C, to reduce its influence on the thermal stability of the PI/SiO_2-OA hybrid composite and maintain good dispersion stability in DMAC, SiO_2-OA-1 was selected as the filler for preparation of the PI/SiO_2-OA hybrid composites (PISA) in the rest of this study.

FTIR spectra of the PI/SiO_2-OA nanocomposites

The FTIR spectra of the PI/SiO_2-OA hybrid nanocomposites (PISA system) with various amounts of SiO_2-OA-1 are shown with that of the pure PI in Figure 6. The characteristic absorption peaks of the

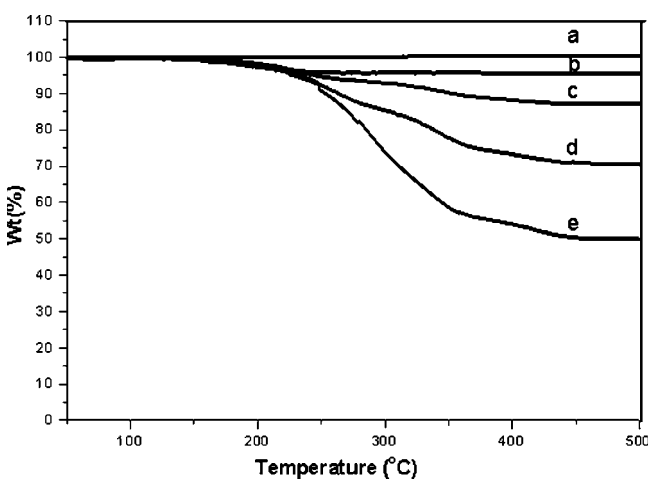

Figure 5 TGA curves of (a) pristine SiO_2, (b) SiO_2-OA-1, (c) SiO_2-OA-2, (d) SiO_2-OA-3, and (e) SiO_2-OA-4.

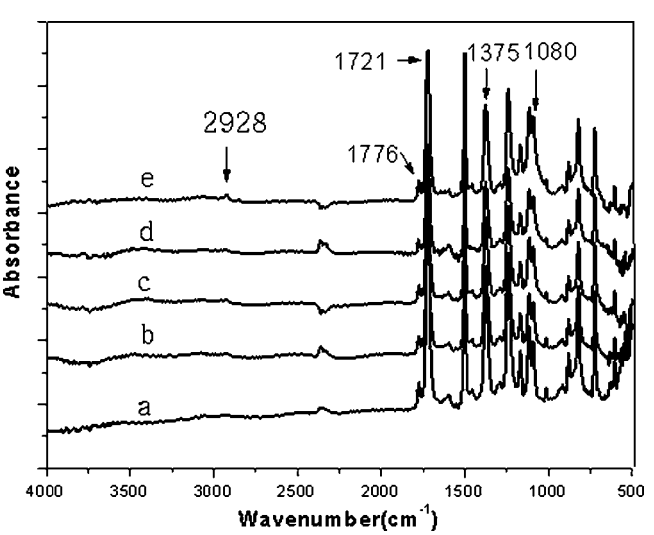

Figure 6 FTIR spectra of (a) pure PI, (b) PISA-3, (c) PISA-5, (d) PISA-7, and (e) PISA-9.

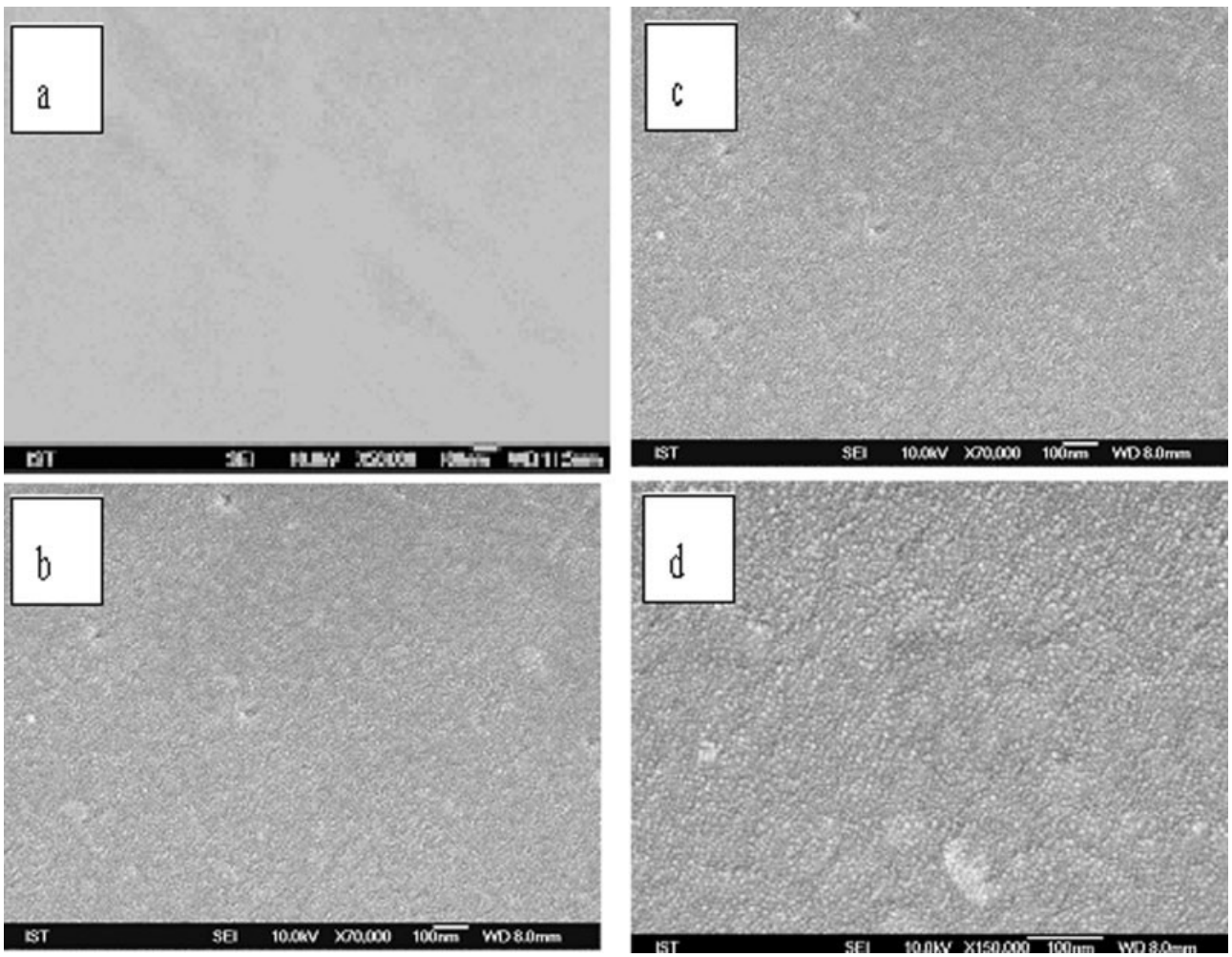

Figure 7 SEM photographs of the surface view for (a) pure PI, (b) PISI, (c) PISA-5, and (d) PISA-9.

pure PI are observed at 1776 and 1721 cm^{-1} for C=O, 1375 cm^{-1} for C—N—C, and 1243 cm^{-1} for ether group, and the peaks of the —O—H group and the —N—H group of the poly(amic acid) are disappeared, indicating that the imidization reaction was completed via the heating process. For the PI/SiO_2-OA-1 hybrid composites, the corresponding characteristic absorption peaks of the PMDA/ODA PI matrix and the SiO_2 micro-domain are observed as expected. Although the OA moiety on SiO_2-OA nanoparticles was unstable before 300°C as mentioned earlier, the characteristic absorption peak for the $—CH_2—$ asymmetrical stretching of the OA moiety at 2928 cm^{-1} for the PISA films are still observable, indicating that at least some of the OA moieties were remained during imidization i.e. the thermal stability of the OA moiety was increased in the as-prepared PISA films. This may be ascribed to the good compatibility and possible interaction of SiO_2-OA-1 with PI matrix. The matrix is considered as a thermal protection for the embedded OA moieties. The enhancement of thermal stability is supported by the TGA measurement discussed below.

Morphology of the PI/SiO_2-OA nanocomposites

The surface and fracture surface SEM photographs of the as-prepared films are shown in Figures 7 and 8, respectively. As shown in Figure 7(b), aggregates are observed on the surface of PISI, the PI/pristine SiO_2 hybrid film, indicating a poor compatibility between the pristine SiO_2 and the PI matrix. However, Figures 7(c) and 7(d) exhibit that the surfaces of the PISA-5 and PISA-9 films are all quite smooth and the SiO_2-OA-1 nanoparticles were well dispersed in the PI matrices. Besides, Figures 8(a–d) show that the fracture surface of pure PI film is extremely smooth, but, a plate-like structure is found perpendicular to the fracture surface for the PI/SiO_2-OA-1 hybrid films, indicating that a fracture

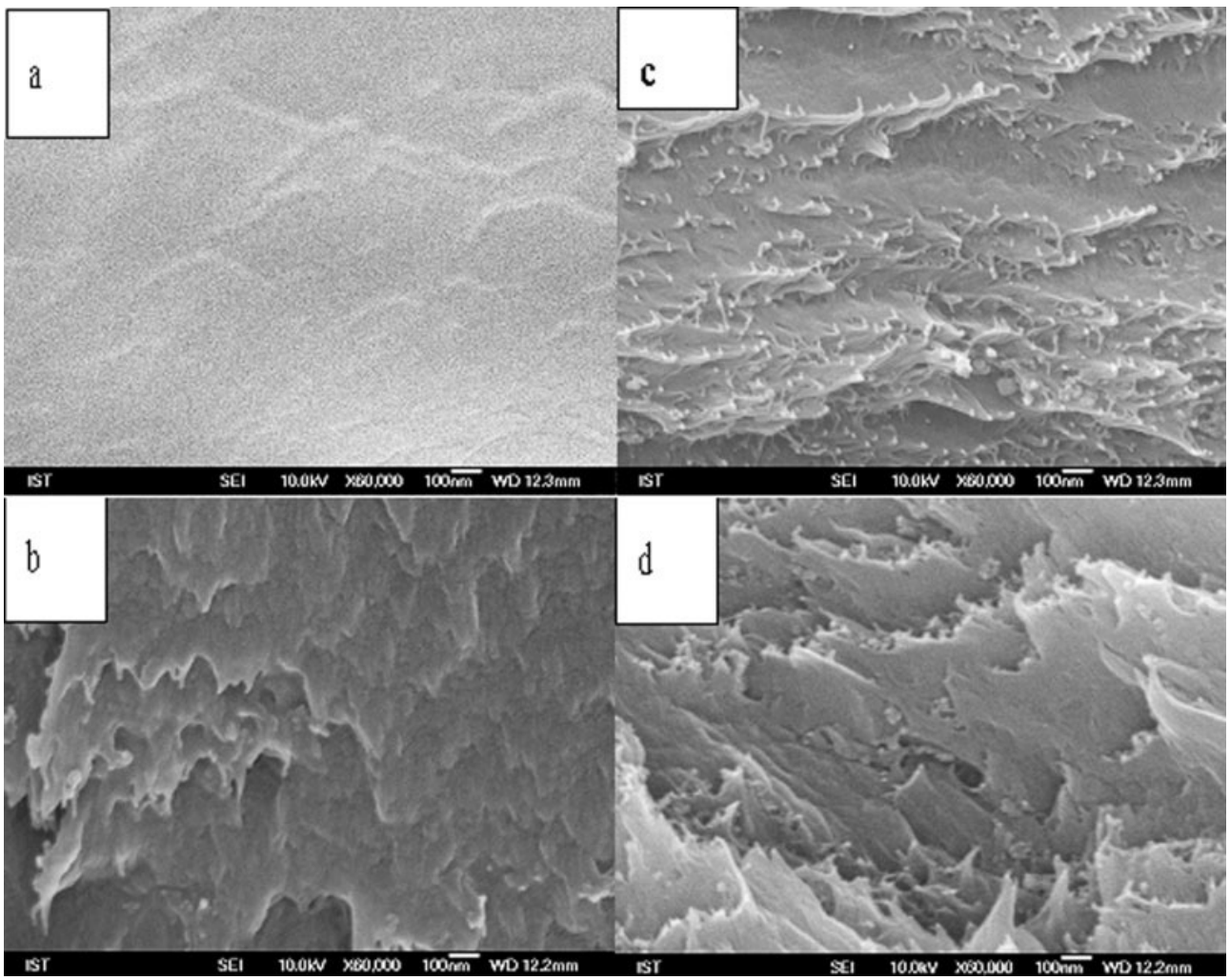

Figure 8 SEM photographs of the fracture surface for (a) pure PI, (b) PISA-3, (c) PISA-5, and (d) PISA-9.

resistance existed in the nanocomposites, which are in a microstructure consisting of nanoparticles and polymer matrices because of the presence of the possible interaction between the nanoparticles and the PI matrix. It is also found that the roughness of the fracture surface is increased with increasing the content of SiO_2-OA-1 nanoparticles. The interfacial characteristics between the nanoparticles and the PI matrix would affect its mechanical property, as discussed in the paragraph below. In addition, the silicon mapping photographs of the surface and the fracture surface of the PISA-9 film shown in Figure 9 indicates that the silicon atoms are quite uniformly distributed in the whole matrix. The results reveal that the SiO_2-OA-1 nanoparticles were much better dispersed in the PI matrix than the pristine SiO_2 nanoparticles as expected. This is ascribed to the good compatibility and the possible interaction of SiO_2-OA-1 with the PI matrix.

Thermal stability of the PI/SiO_2-OA nanocomposites

The thermal properties of the as-prepared films were investigated by TGA in nitrogen atmosphere. The TGA thermograms are shown in Figure 10 and the corresponding data are summarized in Table III. It is seen that the thermal data of PISI are similar to that of pure PI film, while the thermal decomposition temperature ($-T_5$%) of PISA is slightly increased, from 549 to 553°C, and the temperature at maximum weight loss rate (T_{max}) remained around 551°C as the SiO_2-OA-1 content was increased to 9 wt %. This is attributed to the high stability of silica network, well dispersion of SiO_2-OA-1 in the PI matrix and good compatibility between SiO_2-OA-1 and the PI matrix. In addition, the residues remained at 800°C were increased from 57.1 to 61.3 wt % as increasing the SiO_2-OA-1 content as expected. These results indicate that the addition of the SiO_2-OA-1 nanoparticles into the PI matrix slightly

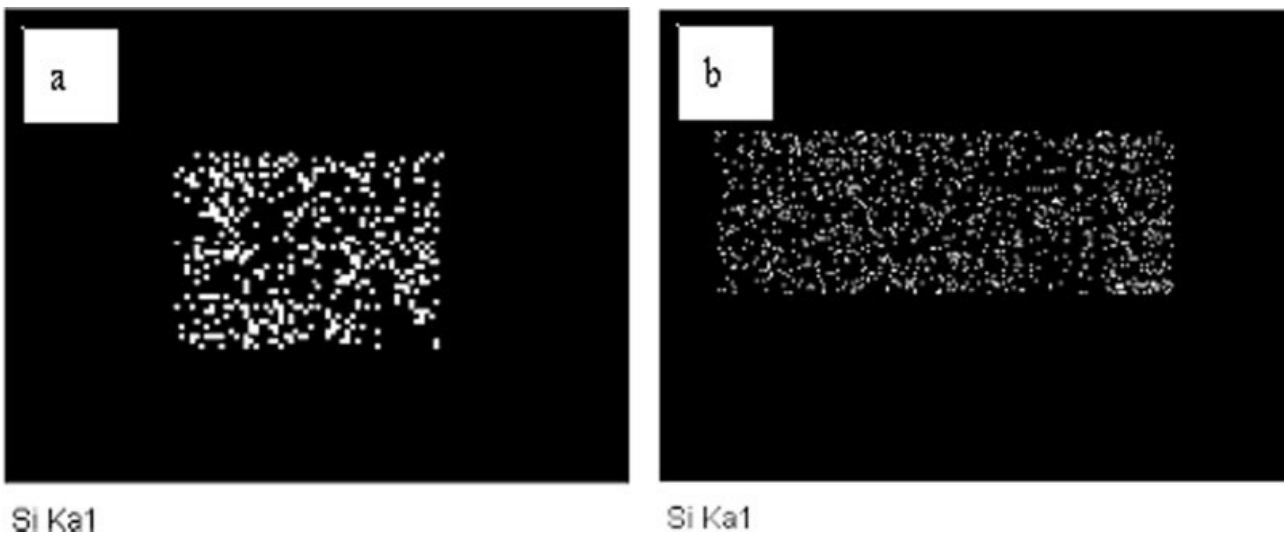

Figure 9 Silicon mapping photographs of PISA-9 (a) top view and (b) cross section.

increase its thermal stability, implying that the OA moieties were thermally stabilized in the PI matrix as evidenced by the IR spectra discussed earlier.

DMA of the PI/SiO_2-OA nanocomposites

The storage modulus and the tan δ curves of the as-prepared films are shown in Figures 11 and 12, respectively. The glass transition temperature (T_g) data taken from the tan δ peaks are listed in Table III. As indicated, the T_g of PI was as high as 394°C and was not obviously affected by addition of the SiO_2-OA-1 or SiO_2. On the other hand, the storage modulus (E′) of the PISA film was significantly enhanced with increasing the SiO_2-OA-1 content in the whole temperature range measured, and was about 110 and 80% increment at 300°C for PISA-9 when compared with PI and PISI, respectively. This is attributed to the existence of the possible interaction between SiO_2-OA-1 and PI.

CTE of the PI/SiO_2-OA nanocomposites

Figure 13 shows the coefficient of thermal expansion (CTE) plots of the as-prepared films in *z*-axis and the data are listed in Table IV. As can be seen, the CTE value of the PISA film was decreased with increasing the SiO_2-OA-1 content, from 27.3 ppm/°C for pure PI to 15.9 ppm/°C (42% lowering) and 15.1 ppm/°C (45% lowering) for PISA-5 and PISA-9, respectively, while that of the PISI film was not significantly lowered by addition of the pristine SiO_2. The effective lowering of CTE for the PISA film is ascribed to the nano-size of the SiO_2-OA-1 particles and well dispersion in the PI matrix[11,13] as well as the inherently low CTE of the SiO_2 network (about

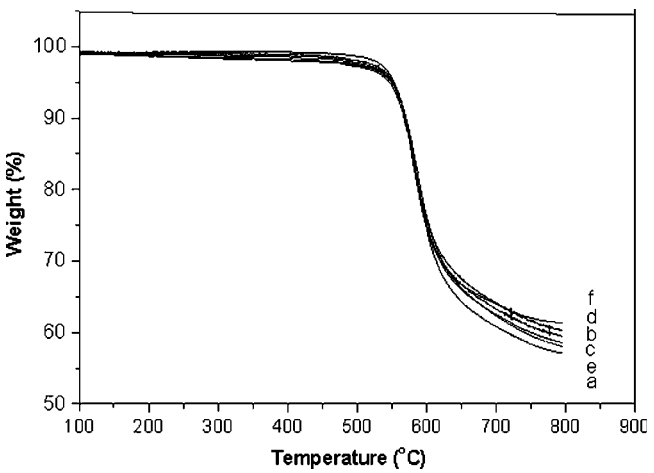

Figure 10 TGA curves of (a) pure PI, (b) PISI, (c) PISA-3, (d) PISA-5, (e) PISA-7, and (f) PISA-9.

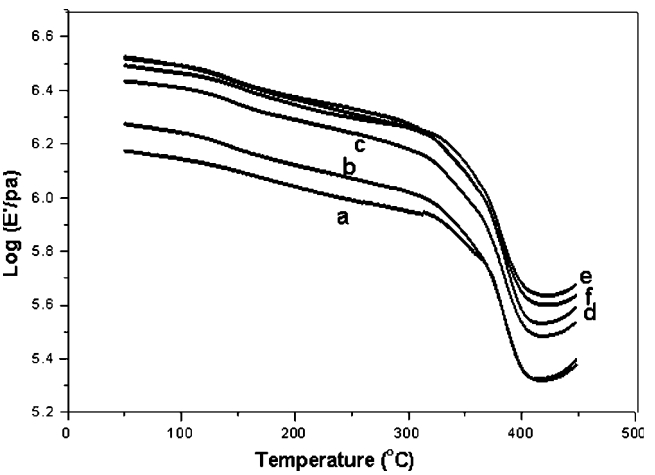

Figure 11 Storage modulus of (a) pure PI, (b) PISI, (c) PISA-3, (d) PISA-5, (e) PISA-7, and (f) PISA-9.

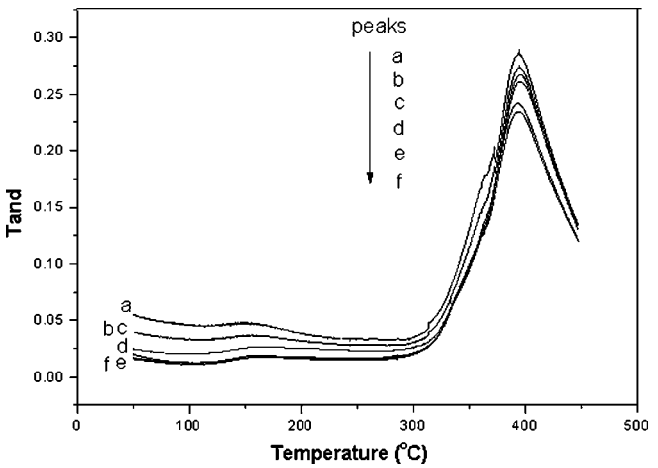

Figure 12 Tan δ plots of (a) pure PI, (b) PISI, (c) PISA-3, (d) PISA-5, (e) PISA-7, and (f) PISA-9.

0.5 ppm/°C), which obstructed the expansion of polymer chains when the temperature is raised. In addition, as reported by Japp and Poliks[28] a CTE close to that of the adhered metal foil, which is 17 ppm/°C for the copper foil, is required to reduce the stress on a solder joint. In this study, the CTE values of the as-prepared PISA films with >5 wt % SiO_2-OA-1 nanoparticles were all quite close to this requirement, implying the potential application in the advanced electronic devices.

Water absorption of the PI/SiO_2-OA nanocomposites

The water absorption data of the as-prepared films are listed in Table IV. It shows that the water absorptions of the PISA nanocomposite films are all less than that of the pure PI film and the PISI film, and is decreased on increasing the SiO_2-OA-1 content, indicating that without the SiO_2-OA-1 filler, water molecules can more easily diffuse into the PI matrix. However, the water diffusion becomes more difficult in the PI hybrid films, especially those containing SiO_2-OA-1 nanoparticles. This is attributed to the hydrophobicity of the SiO_2-OA-1 nanoparticles as discussed earlier.

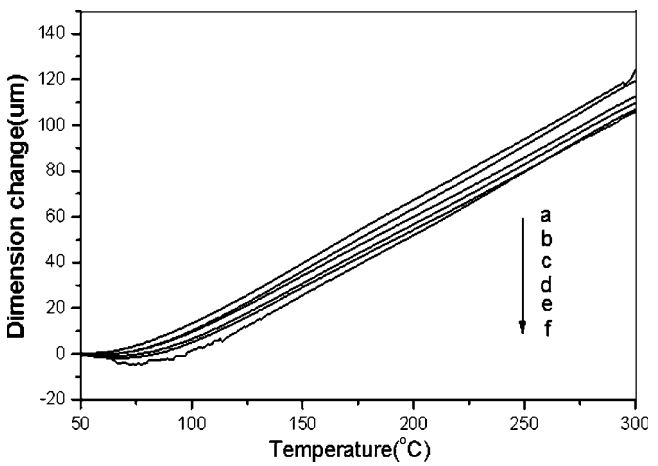

Figure 13 TMA plots of (a) pure PI, (b) PISI, (c) PISA-3, (d) PISA-5, (e) PISA-7, and (f) PISA-9.

TABLE IV
CTE, Water Absorption, and Dielectric Constant Data of Pure PI and the Hybrid Composite Film

Sample	CTE (ppm/°C)	Water absorption (wt %)	Dielectric constant
PI	27.3	3.27	3.62
PISI	24.1	3.06	3.64
PISA-3	22.6	2.81	3.63
PISA-5	15.9	2.58	3.61
PISA-7	15.3	2.19	3.79
PISA-9	15.1	2.05	3.75

Dielectric properties

The dielectric constant of a film is another very important factor for microelectronic applications. However, the dielectric constant may be significantly affected by the morphological structure, crystallinity, chain order, molecular packing, and composition of the materials, including fillers and moisture in the polymer.[29,30] Therefore, the dielectric constants of the hybrid films were also investigated. As shown in Table IV, although the pure SiO_2 has a higher dielectric constant ($\varepsilon' = 3.9$) than the dielectric constant of the pure PI ($\varepsilon' = 3.0$–3.5), the dielectric constants are not significantly affected in the as-prepared PISA films at lower SiO_2-OA-1 (< 7 wt % of SiO_2-OA-1) and SiO_2 loading and are only slightly increased at higher SiO_2-OA-1 loading, compared to the dielectric constant of neat PI.

CONCLUSIONS

A hydrophobic surface-modified nano-sized silica, SiO_2-OA, was prepared via the reaction of the silanol group with the carboxylic group of OA. A series of SiO_2-OA-containing polyimide hybrid nanocomposites (PISA) were then successfully prepared through the dispersion of the SiO_2-OA-1 nanoparticles into the poly(amic acid) solution and thermal imidization reaction. The morphology of the as-prepared PISA films obtained by the SEM and the Si mapping photograph, showed that the SiO_2-OA-1 nanoparticles were uniformly distributed in the PI matrix. The TGA results indicated that the addition of the SiO_2-OA nanoparticles into the polyimide matrix slightly improved its thermal stability. In addition, comparing with pure PI and the pristine SiO_2-containing polyimide hybrid composite (PISI), introduction of the SiO_2-OA-1 nanoparticles into the polyimide matrix effectively lowered the thermal expansion coefficient,

enhanced the storage modulus and reduced the water resistance, but did not significantly affect the dielectric constant. These results indicate that the as-prepared PI/SiO_2-OA hybrid nanocomposites are potential materials for the advanced electronic application.

References

1. Sroog, C. E. J Polym Sci Part D: Macromol Rev 1976, 11, 161.
2. Bessonov, M. I.; Zubkov, V. A.; Polyamic Acids and Polyimides: Synthesis, Transformations, and Structure; CRC: Boca Raton, FL, 1993.
3. Ghosh, M. K.; Mittal, K. L.; Polyimides: Fundamentals and Applications; Marcel Dekker: New York, 1996.
4. Thompson, L. F.; Willson, C. G.; Tagawa, S. Polymers for Microelectronics: Resists and Dielectrics (ACS Symposium Series 537); American Chemical Society: Washington, DC, 1994.
5. Feger, C. Polyimides: Trends in Materials and Applications; Society of Plastics Engineers: New York, 1996.
6. Lu, S. X.; Cebe, P.; Capel, M. Polymer 1996, 37, 2999.
7. Ree, M.; Chen, K. J.; Kirby, D. P. J Appl Phys 1992, 72, 2014.
8. Bellucci, F.; Khamis, I.; Senturia, S. D.; Latanision, R. M. J Electrochem Soc 1990, 137, 1778.
9. Seo, J.; Cho, K. Y.; Han, H. Polym Degrad Stab 2001, 74, 133.
10. Okamoto, K. I.; Tanihara, N.; Watanabe, H.; Tanaka, K.; Kita, H.; Nakamura, A.; Kusuki, Y.; Nakagawa, K. J Polym Sci Part B: Polym Phys 1992, 30, 1223.
11. Southward, R. E.; Thompson, D. S.; Thornton, T. A.; Thompson, D. W.; St. Clair, A. K. Chem Mater 1998, 10, 486.
12. Thompson, D. S.; Thompson, D. W.; Southward, R. E. Chem Mater 2002, 14, 30.
13. Bian, L. J.; Qian, X. F.; Yin, J.; Zhu, Z. K.; Lu, Q. H. J Appl Polym Sci 2002, 86, 2707.
14. Park, C.; Smith, J. G., Jr.; Connell, J. W.; Lowther, S. E.; Working, D. C.; Siochi, E. J. Polymer 2005, 46, 9694.
15. Delozier, D. M.; Orwoll, R. A.; Cahoon, J. F.; Ladislaw, J. S.; Smith J. G., Jr.; Connell, J. W. Polymer 2003, 44, 2231.
16. Magaraphan, R.; Lilayuthalert, W.; Sirivat, A.; Schwank, J. W. Compos Sci Technol 2001, 61, 1253.
17. Agag, T.; Koga, T.; Takeichi, T. Polymer 2001, 42, 3399.
18. Wang, Y. W.; Yen, C. T.; Chen, W. C. Polymer 2005, 46, 6959.
19. Cornelius, C. J.; Marand, E. Polymer 2002, 43, 2385.
20. Huang, Y.; Gu, Y. J Appl Polym Sci 2003, 88, 2210.
21. Kioul, A.; Mascia, L. J Non-Cryst Solids 1994, 175, 169.
22. Yen, C. T.; Chen, W. C.; Liaw, D. J.; Lu, H. Y. Polymer 2003, 44, 7079.
23. Qiu, W.; Luo, Y.; Chen, F.; Duo, Y.; Tan, H. Polymer 2003, 44, 5821.
24. Schrotter, I. C.; SmaihiI, M.; Guizard, C. J Appl Polym Sci 1996, 61, 2137.
25. Ahmad, Z.; Mark J. E. Chem Mater 2001, 13, 3320.
26. Li, Z.; Zhu, Y. Appl Surf Sci 2003, 211, 315.
27. Einsla, B. R.; Kim, Y. S.; Hickner, M. A.; Hong, Y. T.; Hill, M. L.; Pivovar, B. S.; McGrath, J. E. J Membr Sci 2005, 255, 141.
28. Japp, R. M.; Poliks, M. D. U.S. Pat. Appl. US 2002/0050402 A1 (2002).
29. Hong, J. K.; Yang, H. S.; Jo, M. H.; Park, H. H.; Choi, S. Y. Thin Solid Films 1997, 308, 495.
30. Hougham, G.; Tesoro, G.; Viehbeck, A.; Macromolecules 1996, 29, 3453.